About the Michel parameter δ

F. Sobratee

July 10, 2000

Abstract

This report summaries all I know about fitting distribution about the Michel parameter δ. The analysis is done using the package *PAW*(version X11).

Contents

1 Introduction

Our (the E614 analysis team) initial task is to study possible objectives, and make a plan for how to best use our initial beam time with respect to the efficient extraction of physics. (A report is required on August 10.) This report focuses on the extraction of the Michel parameter δ. The next task that will appear in a following report is to look carefully at the effects of systematic uncertainties on δ.

In a Monte Carlo code, the x and the θ values that are generated follow the Michel distribution (neglecting radiative corrections, neutrino and e^+ masses)

$$\frac{d^2\Gamma}{x^2 dx\ d\cos\theta} \sim 3(1-x) + \frac{2\rho}{3}(4x-3) + P_\mu \xi \cos\theta \left[1 - x + \frac{2\delta}{3}(4x-3)\right]. \quad (1)$$

To recall, this equation gives the the differential probability of the decay $\mu^+ \to e^+ + \nu_e + \overline{\nu}_\mu$ to obtain a e^+ with (reduced) energy between x and $x + dx$, emitted at an angle between θ and $\theta + d\theta$ with respect to the muon spin $\vec{P}_\mu$.

$P_\mu = |\vec{P}_\mu|$ is the degree of muon polarization and $x \equiv E_e/\ \max\ (E_e)$ is the reduced energy, where $\max(E_e) = m_\mu/2 = 52.83$ MeV. ρ, ξ, and δ are the Michel parameters with Standard Model values of $\rho = \xi\delta = 3/4$, $\xi = 1$ and $\eta = 0$.

2 Global fit

In the following subsections, no cuts were applied in the analysis of the Monte Carlo data. For the Monte Carlo calculations of the x and the θ values, a subroutine called called zbrent.f [1] (Brent's method) is used for root finding.

Table 1 shows the *global* fit results for 5×10^5 events, without any cuts applied. The duration of the analysis is about 20 seconds. The binning for x and θ is 20 ch. in [0: 1.0] and [0: 3.141593] respectively.

Global fit results with no cuts.	
δ	0.7470±0.0041
ρ	0.7524±0.0021
ξ	1.0053±0.0056
normal. cst	4996±6
χ^2/d.o.f	1.00

Table 1:

A surface plot of the simulated Michel distribution is shown in Figure 1.

2.1 Sensitivity of results to the upper edge for θ

Table 2 shows the sensitivity of the results to the upper value for the binning of the variable θ. The fitting results are when no cuts are applied to the simulated data.

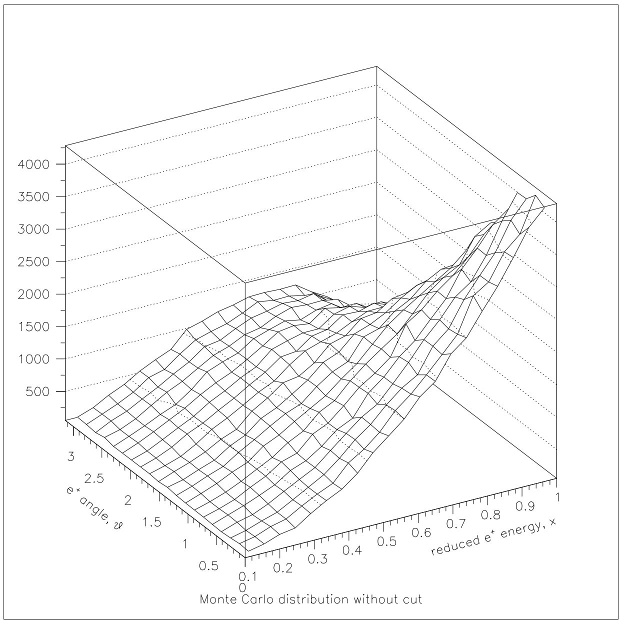

Figure 1: A global fit for 500,000 events.

θ binning	20 ch. in [0: 3.141593]	20 ch. in [0: 3.14]	20 ch. in [0:3.20]
δ	0.7470±0.0041	0.7469±0.0042	0.679±0.003
ρ	0.7524±0.0021	0.7525±0.0021	0.766±0.002
ξ	1.0053±0.0056	1.0058±0.0057	1.138±0.005
normal. cst	4996±6	4993±7	5005±7
χ^2/d.o.f.	1.00	0.98	7.61

Table 2: Note: the binning for x is 20 channels in [0: 1.0].

The same θ binning as in the first column of Table 2 is going to be used from now on.

2.2 Using fine binning.

There is not enough space in memory when 1000 channels are used for both variables x and θ. Table 3 shows the global fit results and the approximate computer time taken for analysing the simulated data for different total number of channels. Figure 2 shows the surface plot for the binning in which 50 channels are used. Compare that figure with Figure 1 in which 20 channels are used. Using much finer binning does not give good fits. From now on the number of channels used is 20. We probably should

# of channels	500	100	50	20
δ	0.728±0.006	0.752±0.004	0.749± 0.004	0.747±0.004
ρ	0.669±0.003	0.770±0.002	0.757±0.002	0.752±0.002
ξ	0.870±0.007	1.023±0.006	1.008±0.006	1.005±0.006
normal. cst	6.68±0.01	196±0	797±1	4996±7
χ^2/d.o.f.	0.74	1.01	0.97	1.01
Analysis time	8 minutes	1 minute	30 seconds	20 seconds

Table 3: The number of channels is for both variables x and θ.

assume that the influence of the granularity of the binning is either a flaw in *PAW*, or in our understanding of the fits. We shall look in that issue later.

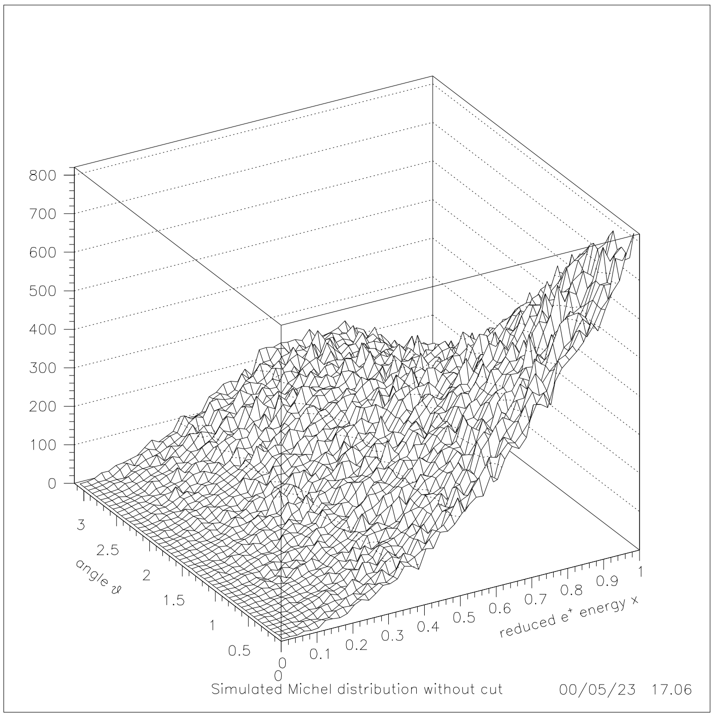

Figure 2:

2.3 Sensitivity of δ to prior knowledge of ρ or/and ξ

Table 4 shows the fitting results with ρ or/and ξ set to its Standard Model value. As a consequence there is no apparent increase in the precision of δ. However the error is reduced by a factor of almost 2.

δ	0.7467±0.0042	0.7501±0.0025	0.7490±0.0022
ρ	set to $\frac{3}{4}$	0.7519±0.0020	set to $\frac{3}{4}$
ξ	1.0035± 0.0055	set to 1	set to 1
normal. cst	4996±6	4996±6	4996±6
χ^2/d.o.f.	1.00	1.00	0.99

Table 4:

3 Sensitivity to the e^+ energy

Perhaps this section is trivial. From Table 5 there is not any conspicuous effect on the result for δ when cuts are applied on the e^+ energy.

cuts	no cuts	x>0.1	x>0.2	x<0.9	x<0.8
δ	0.747±0.004	0.747±0.004	0.748±0.004	0.747±0.004	0.748±0.004
ρ	0.752±0.002	0.752±0.002	0.753±0.002	0.753±0.003	0.753±0.005
ξ	1.005±0.006	1.005±0.006	1.005±0.006	1.004±0.007	1.009±0.012
normal. cst	4469±6	4496±6	3996±6	4497±8	3996±11
χ^2/d.o.f	1.00	1.00	1.10	1.13	1.06

Table 5: Not including low energy positron.

4 Sensitivity to the e^+ angle

Table 6 shows that not including positrons with either large or small angle θ with respect to the muon spin has no remarkable effect on the fit result for δ. Here no cuts was applied to the positron energy, x.

cuts	no cuts	θ>0.2	θ>0.4	θ<3.0	θ<2.8
δ	0.747±0.004	0.748±0.004	0.749±0.005	0.745±0.004	0.746±0.005
ρ	0.752±0.002	0.753±0.002	0.754±0.002	0.753±0.002	0.753±0.002
ξ	1.005±0.006	1.006±0.006	1.005±0.006	1.007±0.006	1.007±0.007
normal. cst	4996±7	4678±7	4358±7	4769±7	4451±7
χ^2/d.o.f	1.01	0.98	1.05	0.97	1.01

Table 6: Here no cuts was applied to the positron energy, x.

When an energy cut of $x > 0.4$ is applied the same conclusion is reached (See Table 7) .

Fit results for 5×10^5 events with $x > 0.4$					
cuts	no cuts on θ	θ>0.2	θ>0.4	θ<3.0	θ<2.8
δ	0.752±0.005	0.754±0.005	0.755±0.006	0.751±0.006	0.750±0.006
ρ	0.752±0.002	0.755±0.002	0.752±0.003	0.752±0.002	0.752±0.002
ξ	1.004±0.006	1.002±0.006	1.001±0.007	1.007±0.006	1.007±0.007
normal.	3339±5	3124±5	2911±5	3187±5	2974±5
χ^2/d.o.f	1.00	1.03	1.11	1.08	1.05

Table 7:

5 The forward and backward e^+ distribution

To consider only forward positrons, the cut applied was: $\theta < \pi/2$. On the other hand for backward positrons, it is:$\theta > \pi/2$. Tables 8 and 9 show the fitting results for these positrons for x in [0:1] and x in [0.4:1] respectively. The precision of δ is one order of magnitude smaller. In both cases, the fit result for δ is more sensitive to the backward e^+'s than to the forward e^+'s.

no cut on x			
cuts	no cuts on θ	forward e^+'s	backward e^+'s
δ	0.747±0.004	0.763±0.015	0.749±0.015
ρ	0.752±0.002	0.750±0.007	0.753±0.006
ξ	1.005±0.006	0.981±0.027	1.007±0.015
normal. cst	4996±7	2509±13	2491±12
χ^2/d.o.f	1.01	1.02	0.97

Table 8:

$x > 0.4$			
cuts	no cuts on θ	forward e^+'s	backward e^+'s
δ	0.752±0.005	0.734±0.017	0.749±0.018
ρ	0.752±0.002	0.756±0.008	0.748±0.007
ξ	1.004±0.006	1.041±0.028	1.005±0.017
normal. cst	3339±5	1657±9	1668±9
χ^2/d.o.f	1.00	1.02	1.11

Table 9:

6 The Anisotropic part of the Distribution and The zero crossing

To eliminate the other Michel parameters, ρ and ξ, the backward distribution (i.e. the distribution for $\theta > \pi/2$) is subtracted from the forward distribution (i.e. the distribution for $\theta < \pi/2$):

$$yield_{forw.} \propto$$
$$x^2 \left[3(1-x) + \tfrac{2\rho}{3}(4x-3) + P_\mu \xi \cos\theta (1 - x + \tfrac{2\delta}{3}(4x-3))\right], \qquad [\theta < \pi/2] \tag{2}$$

$$yield_{back.} \propto$$
$$x^2 \left[3(1-x) + \tfrac{2\rho}{3}(4x-3) + P_\mu \xi \cos(\pi - \theta)(1 - x + \tfrac{2\delta}{3}(4x-3))\right], \qquad [\theta < \pi/2]\ . \tag{3}$$

$$\text{forward-backward yield} \propto x^2 \cos\theta (1 - x + \frac{2\delta}{3}(4x-3)), \quad [\theta < \pi/2]\,. \tag{4}$$

Function plots for forward-backward and the forward+backward yield are shown in Figure 3 and Figure 4 respectively.

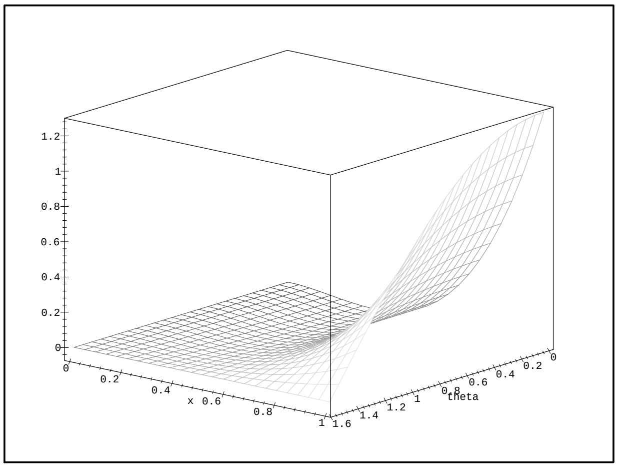

Figure 3: The forward-backward (anisotropic) function plot.

Before going any further, here is a note about the the zero crossing: The zero crossing is the point at which the anisotropic distribution eq. 4 goes to zero. One can easily verify that it occurs at $x_0 = 1/2$. A search for the zero crossing will give us a value for δ by substituting for x_0 in

$$\delta = \frac{x_0 - 1}{\frac{8}{3}x_0 - 2} \tag{5}$$

The associated error in δ is calculated as

$$\delta(\delta) = \delta \sqrt{\frac{(\delta(x_0))^2}{(x_0 - 1)^2} + \frac{(8/3 * \delta(x_0))^2}{(\frac{8}{3}x_0 - 2)^2}}.$$

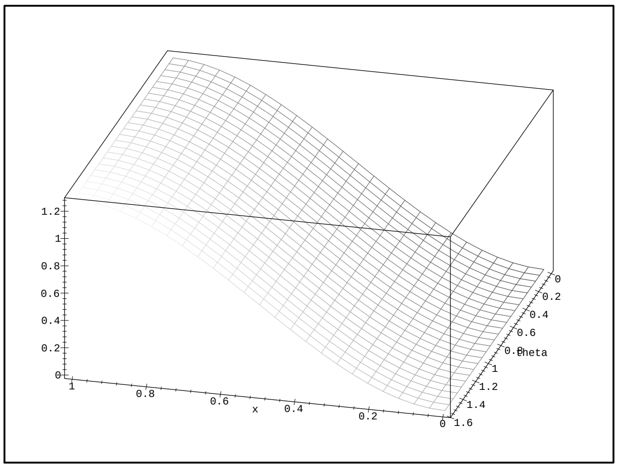

Figure 4: The forward+backward (isotropic) function plot.

End of note.

The simulated anisotropic 'forward-backward' distribution is analysed as follows:

- The forward and the backward distribution are projected into one-dimensional histograms with respect to the e^+ energy x. The binning used is 500 channels for x in [0:1].
- The latter is then subtracted from the former, and the resulting histogram is filled into two vectors, one containing the number of counts and the other the energy x.
- A vector of errors for the forward minus the backward (f-b) distribution is created - the error for a particular channel, is equal to the square root of the sum of the forward and the backward counts in the channel. A plot of the distribution is shown in Figure 5.
- A vector fit is done using the equations:

$$function = par(1) \times x^2 (1 - x + par(2) \times \frac{2}{3}(4x - 3)), \tag{6}$$

  to obtain δ from parameter par(2); and

$$function = x^2 (par(1) * x - par(2)), \tag{7}$$

  to obtain the zero crossing x_0, from which δ will be determined.

Table 10 summarises the results. The value of the zero crossing is $x_0 = 0.5004 \pm 0.0090$.

6.1 More Analysis at the Zero Crossing

In this section, we are going to look closely at the positron decay distribution near the zero crossing. One-dimensional histograms are used since the positron distributions are analysed as a function of θ.

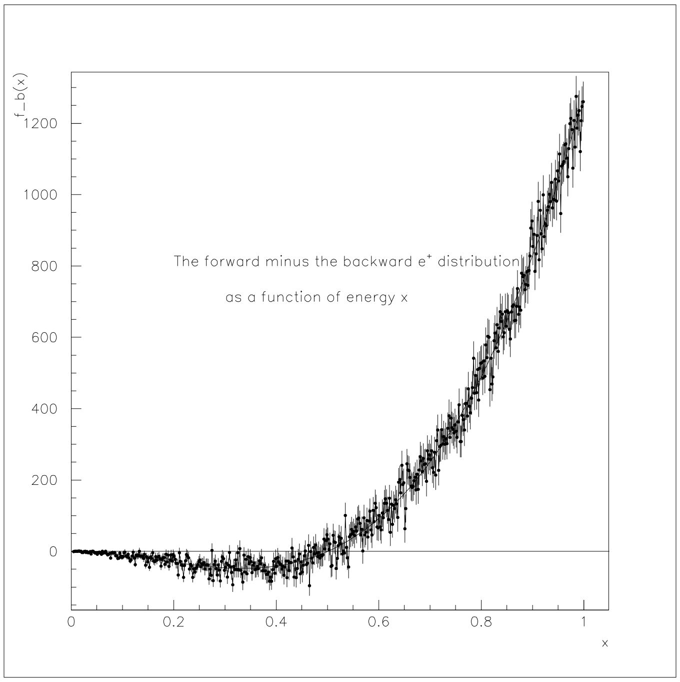

Figure 5:

method	using eq. 6	from x_0 found from eq. 7
δ	0.7506±0.0046	0.7506±0.0304
χ^2/d.o.f for curve fit	0.9324	0.9324

Table 10: Note: the # of channels for x in [0:1.0] is 500.

Since the E614 resolution in x limits the binning to $dx = 0.004$ at the smallest, energy cuts of sizes $\Delta x = 0.005$ were applied to the 'forward-backward yield' at different energies x about the zero crossing. The number of events generated were 500,000 for each energy range. The Monte Carlo data were histogrammed with respect to θ and were fitted to the function

$$\text{function} = a + b\cos(\theta), \tag{8}$$

where a and b are values that depend on the energy range.

Table 11 shows the fit results for a and b for different energy intervals of sizes 0.005. Some 'forward minus backward' angular distribution plots are shown in Figure 6.

The fit was done using the ve/fit command. The histogram of the 'forward minus backward' angular ditribution is copied into two vectors containing the angle θ and the number of counts. A vector of errors for the forward minus the backward angular distribution (which, for a particular channel, is equal to the square root of the sum of the forward and the backward counts in the channel) is accounted for in the fit.

Figure 7 and 8 show the variation of b with x. The straight line fit for the 21 data points gives exaggerated errors. On the otherhand the errors are smaller for a third order polynomial fit with 180 data points. Table 12 summarizes the results from the

energy range	a	b	χ^2/d.o.f.
x in [0.4825, 0.4875]	0.070±3.246	-14.026±4.592	1.19
x in [0.4875, 0.4925]	-4.245±3.247	-2.018 ±4.592	0.96
x in [0.4925, 0.4975]	-6.288±3.248	0.034 ±4.593	1.04
x in [0.4975, 0.5025]	-1.444±3.249	2.224±4.592	0.94
x in [0.5025, 0.5075]	2.412±3.248	-0.512±4.593	1.03
x in [0.5075, 0.5125]	-1.451±3.247	10.945±4.592	0.97
x in [0.5125, 0.5175]	-2.061±3.244	14.664±4.590	0.87

Table 11: Note that the # of channels for θ in [0:$\pi/2$] is 500.

graphs.

# of data points	type of fit	χ^2/d.o.f.	x_0	δ
21	P1	1.09	0.499±0.024	0.748±0.080
180	P3	2.63	0.5039±0.0075	0.756±0.026

Table 12:

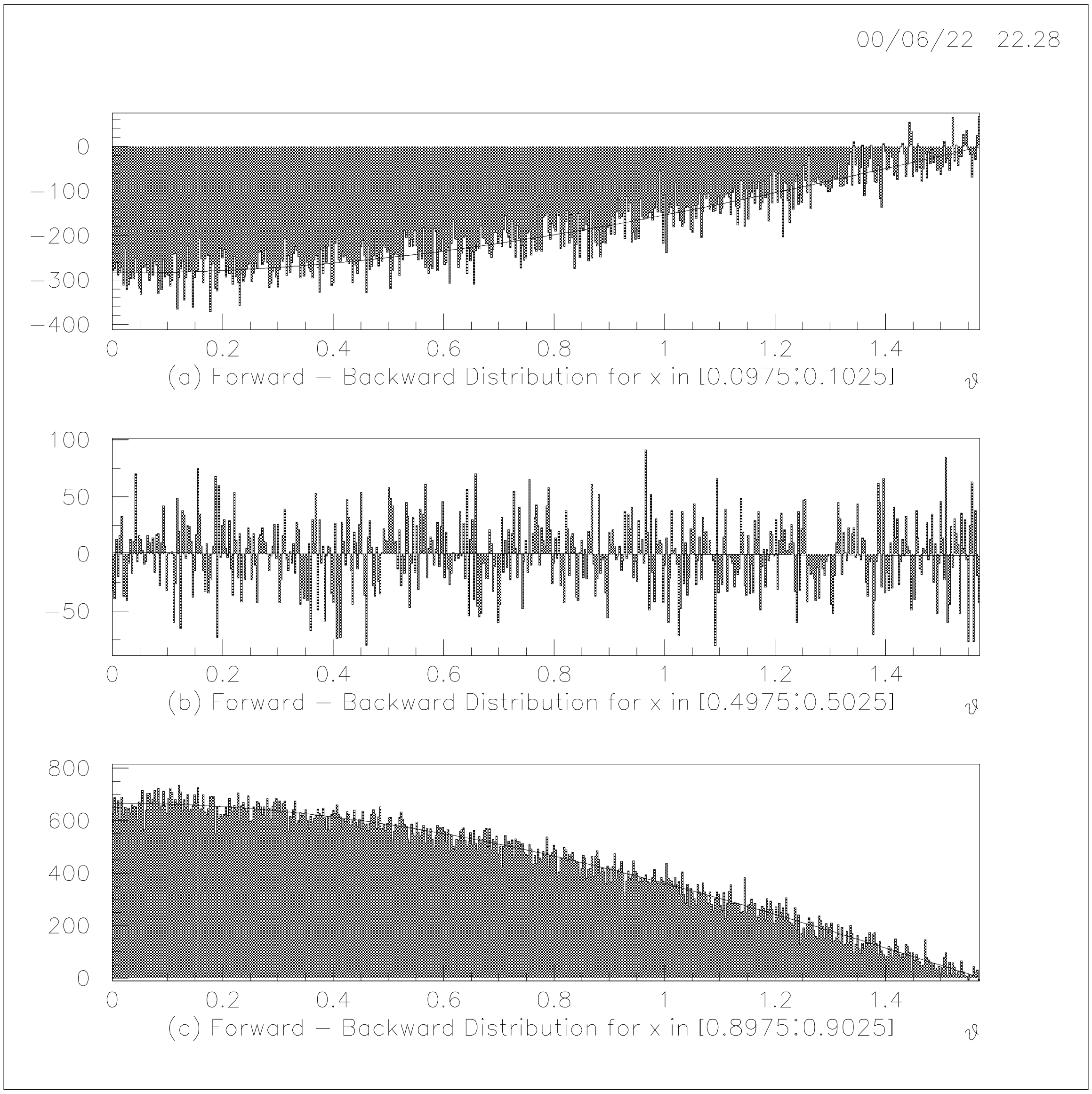
00/06/22 22.28
(a) Forward − Backward Distribution for x in [0.0975:0.1025]
(b) Forward − Backward Distribution for x in [0.4975:0.5025]
(c) Forward − Backward Distribution for x in [0.8975:0.9025]
ϑ

Figure 6:

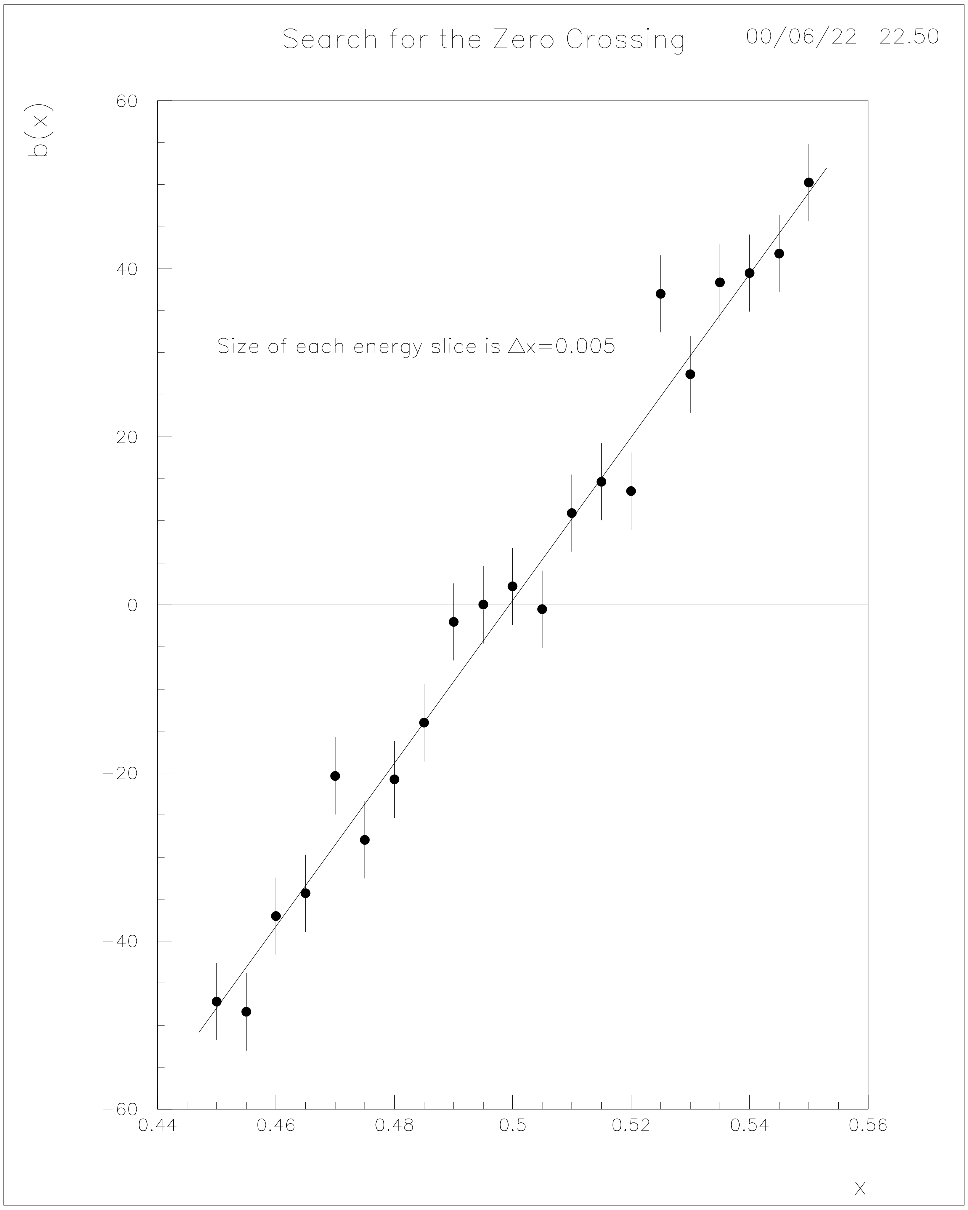

Figure 7: Linear fit with 21 data points.

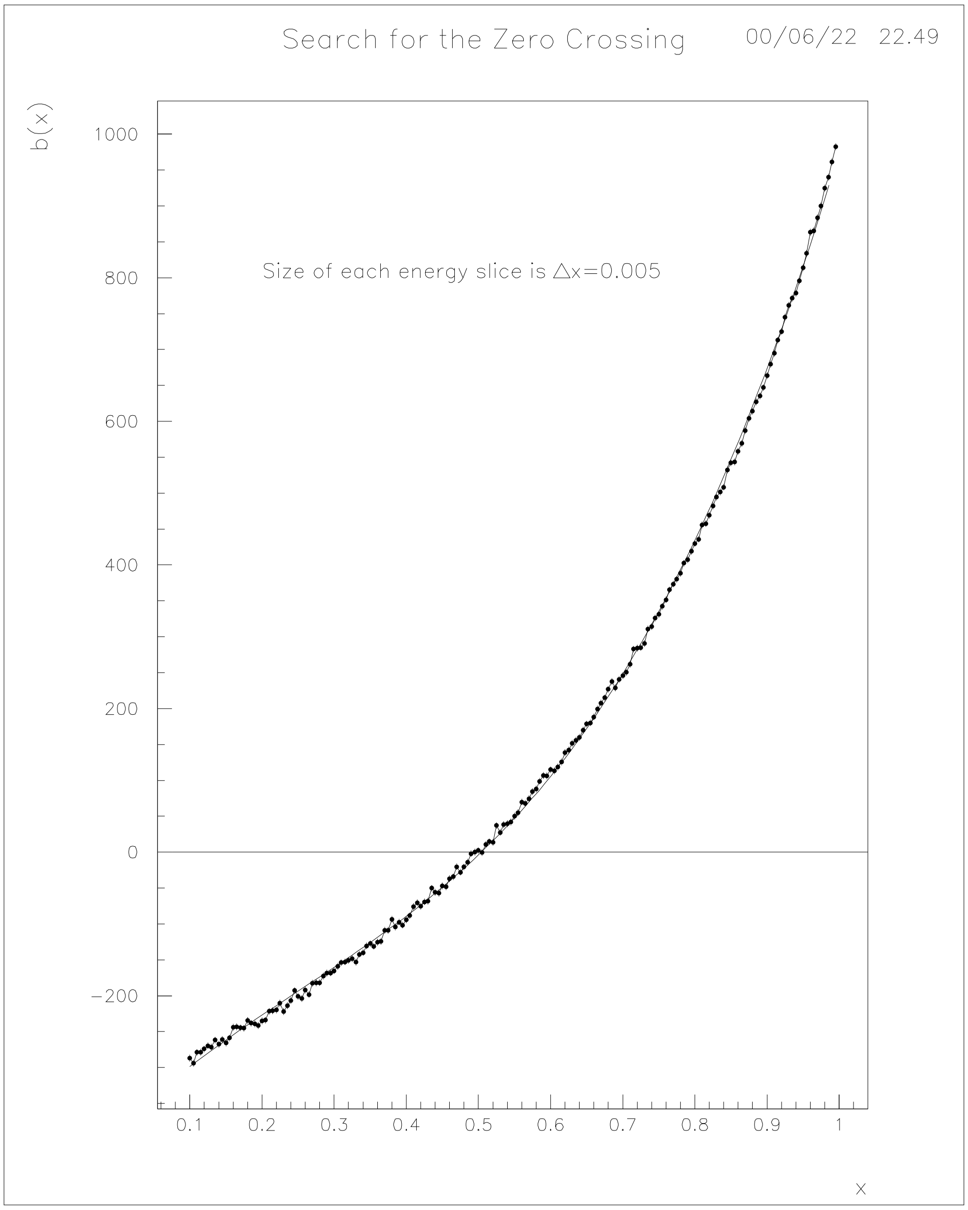

Figure 8: Third order polynomial fit with 180 data points.

References

[1] W. H. Press, B. P. Flannery, S. A. Teukolsky, W. T. Vetterling, *Numerical Recipes, the Art of scientific computing (Fortran Version)*, Cambridge University Press, 1989, page 253.

[2] H. Gould and J. Tobochnik, *An Introduction to computer Simulation Methods* , New Yo rk: Addison Wesley, 2nd Edition, 1996.